A SIMPLE METHODOLOGY TO MEASURE THE DYNAMIC FLEXURAL STRENGTH OF BRITTLE MATERIALS

A. Belenky and D. Rittel (*)

Faculty of Mechanical Engineering
Technion, Israel Institute of Technology
32000 Haifa, Israel

Abstract:

A simple methodology is proposed for measuring the dynamic flexural strength of brittle materials. The proposed technique is based on 1-point impact experimental setup with (unsupported) small beam specimens. All that is needed is a measurement of the prescribed velocity as a boundary condition and the fracture time for a failure criterion, both to be input in a numerical (FE) model to determine the flexural strength. The specimen was modeled numerically and observed to be essentially loaded in bending until its final inertial failure. The specimen's geometry was optimized, noting that during the very first moments of the loading, the specimen length does not affect its overall response, so that it can be considered as infinite. The use of small beam specimens allow large scale testing of the flexural strength and comparison between static and dynamic loading configurations. Preliminary experiments are presented to illustrate the proposed approach.

* Corresponding autor: merittel@technion.ac.il

KEYWORDS: brittle material, dynamic flexural strength, 1-point impact

1. Introduction

The wide usage of ceramic materials in many highly demanding engineering applications has increased the need for reliable measurements of their mechanical properties. Much work has been done on this subject concerning static loading. Several standardized techniques are available for testing the mechanical properties of advanced ceramic materials such as flexural strength [1], compressive strength [2] and static fracture toughness [3]. It is also well known that brittle materials, such as ceramics, possess a significantly higher compressive strength than its tensile counterpart. This observation has been rationalized in terms of the internal flaws that are less active in compression than in tension. Consequently, knowledge of the tensile strength of a ceramic is of prime importance to the designers' community. While compressive testing (either static or dynamic) is a relatively straightforward task, tensile testing is a real challenge, would it only be for the fact that the results are very sensitive to specimen alignment issues.

Moreover, many situations involve dynamic loadings of ceramic components, and here, there is an obvious lack of simple and reliable procedures for testing these brittle materials. In this work, we will concentrate on the assessment of the dynamic tensile (flexural) strength of brittle materials.

Dynamic compression of brittle materials drew much attention in the recent years, because their compressive strength is very high added to their pressure-sensitivity [4] Since these materials are widely integrated into armor applications, much work has been done on the determination of compressive (confined) strength and their fracture modes.

Concerning tensile testing, one should note that most researchers tend usually to avoid direct tensile testing configurations, in both, static and especially dynamic loading regimes. The main reasons for that lie in the high cost of machining and manufacturing specimens, gripping and alignment issues which all complicate the experimental setup. Consequently, several indirect tensile testing techniques have been devised, which are applied to both static and dynamic testing. One of the widely adopted experimental approaches to determine tensile strength of brittle materials is the so-called Brazilian disk specimen configuration. In these test a disk specimen is diametrically compressed. Failure is being caused by an induced tensile stress in the middle of the disk [5]. The ASTM C1144 [6] standard suggests a test method to measure static splitting tensile

strength of brittle materials. Some limitation is mentioned in this standard testing procedure, namely: the stress state tends to be biaxial and loading pads should be used in order to prevent compressive-stress failure near the loading points. To avoid biaxiality in Brazilian disk tests, the ring test was suggested [7]. The ring test differs from the Brazilian disk by a hole that drilled in the center of the specimen, thus causing a more tensile stress state. However, severe doubts were raised about the validity of tensile strength values calculated by this method by Hudson [7]. In order to prevent compressive-stress failure near the loadings points, several improvements were introduced. These include a modified Brazilian disk, when the difference consists of arc-shaped steel spacers in order to evenly distribute the loading over a wider area [8]. Another version consists of a flattened Brazilian disk specimen [9] that partially solves the loading problem, but has some other limitations [8]. In general it is possible to reduce the contact stresses by loading the Brazilian disk between curved anvils or fitting a relatively soft washer in the contact areas, as also suggested by standard for static loading [6]. Yet, in the case of dynamic loading, impedance mismatch and reproducibility issues arise and the accuracy of the experimental results is decreased [10].

Another technique to determine the dynamic tensile properties is the spalling test. Usually, this technique consists of projecting a plate of the investigated material against a rigid flat target. On impact, compressive stress waves originate and reflect from the back surface of the plate as tensile waves, thus inducing spalling [10]. A modification of this technique uses a long cylindrical rod and the experimental setup consists of a Split Hopkinson Pressure Bar (SHPB) [11]. In both specimen configurations (plate and cylindrical rod), a rather significant piece of investigated material is needed, which is not always available. Spalling tests are also difficult in terms of data processing [11].

The bend test provides a convenient alternative, both in terms of specimen manufacturing, experimental setup and data reduction, to calculate the flexural (tensile) strength. One of the proposed specimen's is the semicircular bend specimen (SCB) that can be loaded by a SHPB in three-point bending configuration [12]. This specimen is simply a half of the Brazilian disk specimen, and the three-point configuration loads it in bending. There are some advantages in such configuration, however it still has the same limitation as the Brazilian disk specimen, in addition to the fact that modeling

such a configuration is rather complex, in addition to the requirement for dynamic specimen equilibrium.

The purpose of present research is thus to determine the dynamic flexural strength of advanced ceramics using flexural testing, yet keeping it to the simplest possible level. The overall approach is largely simplified by the observation that under impact conditions, the specimen's failure occurs inertially so that the specimens does not need to be supported, which in turn greatly facilitates its modeling as discussed in the sequel. The experimental technique called 1-point (bend) impact was used in several instances related to dynamic fracture mechanics. One should mention here the work of Böhme and Kalthoff [13], where these authors found that in early stage of the 3-point bending test, the supports do not influence the loading and the loading histories for specimen with or without support is identical.

The proposed technique consists therefore of 1-point impact tests of unsupported specimens (such as beams), as described e.g. by Weisbrod and Rittel [14], or by Rittel et al. [15]. More recently, Belenky et al. [16] applied the one-point impact technique to measure the dynamic initiation fracture toughness of nanograined transparent alumina. In other words, the state of development of the proposed technique and its related modeling aspects are quite advanced for dynamic fracture problems, so that it can almost be applied in a routine fashion to strength testing with minor modifications.

At this stage, one should note the very recent work of Delvare et al. [17], who developed a full dynamic bending test of brittle beams to assess their flexural strength. The idea is to use a model of the dynamic response of the beam to assess its strength on the one hand, while failure is identified from the experimental signals. Specifically, since a set of Hopkinson bars (one incident + 2 transmitted) are used, the reflected signal in the incident bar is used to assess the onset of dynamic fracture. These authors verified their method on relatively long beam specimens (of the order of 20 cm). While the proposed method is quite elegant, its practical implementation relies on a sophisticated dynamic bench test on the one hand, but also on specimens that are quite large, to an extent that is not always practical with ceramic materials. Moreover, as will be shown in the sequel, when the specimen's dimensions are reduced, it is almost impossible to detect variations in the reflected signal that would unambiguously signal fracture. But the most interesting point is that these authors remark that fracture occurs

in an inertial manner, as noted previously, which indicates that supports are not really necessary.

We now propose to implement the one-point impact technique to the assessment of the dynamic flexural strength of brittle materials, noting that in this case the specimen will not be pre-cracked. The specimen size will be kept as small as possible. Here one only needs to measure the boundary conditions, namely applied displacement/velocity (and perhaps load), as well as the fracture time signaled as before by a single wire fracture gauge [14]. The approach is of a hybrid experimental-numerical nature in which the boundary conditions and fracture time are applied to a linear elastic numerical (finite element) model of the experiment.

In the following section we will present the numerical model of the experiment, including considerations about specimen's size. Next, we will describe an experimental illustration of the proposed technique, followed by a discussion section and concluding remarks.

2. Specimen and numerical model

2.1 Specimen design considerations

Machining of ceramic materials is quite delicate, in addition to the fact that the quantity of available material is often limited, so that specimen dimensions and machining should be carefully optimized. The proposed short-beam geometry allows convenient pre-shaping in a green (powder) form, sintering and grinding in order to get good surface finish and accurate dimensions. The ASTM C1161 standard [1] suggests three different specimen's sizes for flexural testing of advanced ceramics. The preparation method, along with prescribed tolerances and surface finishing also defined in this standard. Therefore, in order to use same specimens for both type of loading (static and dynamic) while minimizing high-cost unnecessary machining, it was decided to follow the standard recommendations [1] for specimen's dimensions and shape, as shown in Figure 1.

2.2 Numerical model

In order to prove that the stress distribution in the short-beam specimen during impact is characteristic of bending, a simple numerical model was created using the commercial finite element code ABAQUS 6.8-2 [18]. The model was built based on 1-point impact

technique as described in Weisbrod and Rittel [14] and implemented by these authors for dynamic fracture toughness measurements of tungsten based heavy alloy as well as by Belenky et al. [16] for transparent nano-grained alumina. The 1-point impact experimental setup is shown in Figure 2, and it consists of three components, namely incident bar (and striker), specimen and fracture gauge. The specimen boundary conditions during an impact are free-free, thus reducing the complexity of the finite element model. Half-model with one symmetry condition was used to investigate the dynamic stress distribution in the specimen, as shown in Figure 3. The modeled incident bar dimensions is ø6.35x500 [mm] and the specimen is 3x4x45 [mm^3], as suggested by [1]. The striker velocity profile, as in ordinary Split Hopkinson (Kolsky) Pressure Bar (SHPB) test, was implemented as a loading condition, Figure 4. We chose to model commercial alumina whose physical properties are listed in Table 1, in addition to those of the steel bar material (15-5PH).

Numerical convergence was checked on both, the incident bar and specimens models. A meshed model along with the boundary conditions is shown in Figure 5. The number of elements, their type and other relevant details are all listed in Table 2. It was previously shown by Giovanola [19] and by Rittel et al. [15] that an impacted unsupported structure will not immediately start to propagate away from the contact point upon impact. Rather, a certain amount of time will elapse, during which loading waves travel back and forth in the structure. These authors used in their studies notched/cracked specimens and their conclusion was that the structure fractures long before the specimen takes off from the contact with the incident bar. In this study specimens don't have notches/precracks, so that the loading causes inertial bending only, until fracture.

2.3 Numerical results

A typical stress distribution on the outer (tensile) surface of the specimen (Figure 6a) is shown in Figure 6b. From Figure 6b it is clear that the bending stress (S_{11}) prevails most of the time during the one-point impact test. The other stress components (S_{22} and S_{33}) have no influence during the initial phase of the loading, and essentially keep a very low level as compared to S_{11}. For the sake of completeness, the Mises stress is also plotted on this figure, and from the comparison of Mises and S_{11} curves, one can note that the shear stress components (not shown in this plot) have a minor influence, if any. This plot proves that uncracked short-beam specimens loaded by 1-point technique will essentially experience bending stress which will ultimately cause failure.

Finally, the local strain-rate $\dot{\varepsilon}$ was found to be $\dot{\varepsilon} \approx 450\left[s^{-1}\right]$ for a steel bar, while it became $\dot{\varepsilon} \approx 900\left[s^{-1}\right]$ for an aluminum bar, emphasizing the role of the mechanical impedance on the expected strain rate. In this context, one should pay attention to the accuracy of detection using the single wire fracture gauge. For the above mentioned strain-rates, the accuracy of determination of the stress will be $166\left[MPa/\mu s\right]$ and $332\left[MPa/\mu s\right]$ respectively for this material. Consequently, care should be paid to silk-screen narrow fracture gauges, as shown in Figure [10]. This point is further addressed in the experimental section.

2.4 Preliminary optimization of the specimen's geometry

In order to optimize the specimen's geometry several specimens' sizes were checked numerically. The incident bar diameter was kept constant to reflect our experimental setup (ø6.35 [mm]), so that the smallest specimen size suggested by ASTM C1161 [1] was considered. However, it was found that this specimen is not practical in terms of experimental positioning and difficulty in laying out a fracture gauge.

Numerical simulations were therefore run for three of specimens' cross-sections: 3x4, 4x5, and 5x6 [mm^2], where the larger side (d) of the specimen's cross-section is in contact with the incident bar. For each cross-section, various specimen lengths were checked numerically. Figure 7 shows three different specimens' geometries, for which the ratio between the depth (d) of the specimen to its length (L_t) was kept constant, (~0.09, Figure 1). During the first 12 [μs] of the loading, the bending stress on the outer surface of the specimens is almost identical for all specimens geometries. Thereafter, different bending stress curves are obtained for each specimen. These differences can be attributed to wave's reflection from the longitudinal ends of the specimen. In other words, for the first 12 [μs] of the loading after the stress wave reaches the specimen, the specimens basically behave as infinite. A similar observation was also reported in Delvare et al. [17] from much larger specimens.

2.5 Failure simulation

In order to gain some qualitative understanding of the specimen's failure, a maximum principal stress (Rankine) failure criterion was implemented as a user-subroutine [18]

and introduced into the numerical simulations. This failure criterion uses the stress data at integration points of each element, calculates the maximum principal stresses, and erases elements when a certain critical stress level (flexural strength) is reached. The only input into this subroutine is the value of flexural strength of the tested material. In the present simulations, the maximum principal stress value was set to 400 [MPa], a representative value for commercial alumina (Table 1).

The simulation results are shown in Figure 8. The time reference is the same as in Figures 6-7, and it is set with to t=0 [μs] when the stress wave just impinges on the specimen (Figure 8a). Figures 8b-c show the maximum stress distribution at t=5 and t=7 [μs] respectively, after the stress wave reached the specimen. Note that the specimen has not failed yet. From Figure 8d (t=8 [μs]), it can be observed that as the maximum principal stress reaches the level that was set for elements deletion, failure proceeds from the outer (tensile) surface of the specimen (marked by red circle). Failure happens long before the specimen looses its contact with the incident bar. Figures 8e-f show complete failure of the specimen, with additional cracks being formed on both sides of the specimen, Figure 9. It is interesting to note here that a similar failure pattern was observed by Dorogoy and Rittel [20] in the totally different context (plastic hinges) of the dynamic response of aluminum beams subjected to 1-point impact.

3. Experimental

Experimental validation of the proposed technique was made on three ceramic specimens that were available in our laboratory. Since their exact composition was unknown, it was identified using SEM-EDX technique and found to contain Si, C, Al and N. Yet, this observation was not sufficient to firmly identify the ceramic material and mostly its fabrication process. Consequently, the reported experiments are of a qualitative nature aimed at validating the approach rather than at providing accurate strength data for this material.

The specimens' (beam) dimensions were 3x4x45 [mm^3]. Silver paint fracture gauges were silk-screened on the outer (tensile) surface of each specimen, as shown in Figure 10. The incident bar was, as mentioned, made of 15-5 hardened PH steel with a diameter of ø6.35 [mm] and length of 660 [mm]. The strain gauges were positioned at 395 [mm] from the end of the incident bar that is in contact with the specimen. This was

done in order to get enough time for triggering the high-speed camera and the flashes, so they reach their full lighting power.

A total of 16 high-speed pictures were made during each experiment, using our Cordin 550-16 high-speed camera at framing rates between 110 to 150 [kfps]. The camera was triggered by the incident strain gauge signals, set up to a level of 3.5 mV, Figure 11.

By checking the incident ε_{in} and reflected ε_{ref} signal from the actual test (Figure 11), one can note that they do not differ significantly, so that the measured load, $\propto\left(\varepsilon_{in}+\varepsilon_{ref}\right)$, is too noisy. Consequently, a measured displacement/velocity, $\propto\left(\varepsilon_{in}-\varepsilon_{ref}\right)$, is preferable, since of a much higher precision. Note that this situation is the result of the specific acoustic impedance mismatch which results from the combined bar-specimen geometry. In other instances, e.g. [17], the incident and reflected signals are quite different for a much larger specimen geometry.

The fracture gauge reading and the exact time of each picture were synchronized according to incident signal. In order to do so, the wave velocity in the bar and time at which the wave reaches the specimen were determined from the duration roundtrip of the signal in the bar. For the sake of brevity, we will just describe one experiment out of 3 for this kind of specimens, keeping in mind the results were highly repeatable.

Concerning the above-mentioned accuracy of the fracture-gauge reading, one should mention that the sampling was carried out at a rate of 10 [MHz]. From Figure 11, the rise time of the fracture-gauge signal from zero to its maximum value (full fracture) was found to last for some 2 [μs]. However, due to the high sampling frequency, a clear variation in the level of the fracture gauge signal could be detected after 100 [ns]. Consequently, a representative error in the determination of the flexural stress is of the order of 17 or 34 [MPa] for the above mentioned values of the local stress-rates of $166\left[MPa/\mu s\right]$ and $332\left[MPa/\mu s\right]$ respectively. For a typical strength of 400 [MPa] this error corresponds to 4.25 and 8.5 [%] respectively, which is not too large.

Figures 12-15 shows selected pictures from shot Sp4. The framing rate in this test was 112676 [fps]. Figure 12 shows the beginning of the 1-point test, at t=9.25 [μs] from the time at which the stress wave impinges upon the specimen. The synchronized fracture gauge reading is t_f=9.92 [μs]. So the first reported picture was taken just before

specimen's failure. Figure 13 shows the picture right after fracture occurred, at t=18.12 [μs]. This picture shows that the specimen has failed and cracked into two halves, but it is still in contact with the incident bar. In addition, small crack starts to develop just above the upper fracture gauge's tab. The next high-speed picture, Figure 14, is taken at t=27.00 [μs]. The main central crack is fully developed and the central part appears to bend significantly. The crack above the upper fracture gauge's tab is also clearly seen. If one qualitatively compares numerical simulation results (Figure 9) and experimental failure pattern (Figure 14), they are found to be quite similar indicating a reliable numerical simulation procedure. An additional picture, taken at t=89.12 [μs], shows the total fracture of the specimen and loss of contact with the incident bar, Figure 15. On this figure, the thin layer of lubricant between the specimen and the incident bar is clearly visible.

4. Discussion

This work presents a simple procedure for the determination of dynamic flexural (tensile) strength of advanced ceramics and other brittle materials. The proposed technique is of a hybrid experimental-numerical nature. The experimental setup is a regular Split Hopkinson Pressure Bar and the specimen is of the beam type. In order to create a reliable numerical model, one only needs to know a-priori the Young's modulus, Poisson's ratio and density of tested material. The only boundary condition is the measured velocity/displacement prescribed to the specimen. The last required important information is the fracture time. The latter is measured by means of a fracture gauge, which can also be compared to high speed recording of the test. However, this comparison is not compulsory as a good agreement was observed between the fracture gauge reading and the high speed camera record. With the above-mentioned experimental data, one can construct a simple numerical model which calculates the bending stress experienced by the specimen at fracture time.

One should note that the main advantage of the proposed technique is its simplicity and economy of tested material, a point that is not always fully appreciated in the literature. As such, it allows for large scale testing of brittle materials whose strength is usually statistically distributed. A further simplification can be gained if identical specimens are tested. In this case, all that is needed is the calculation of the specimen's response to a unit displacement (or load) pulse, which can thus be convoluted with the actually

measured displacement or load, again until fracture (linear problem). A similar approach was already used in fracture mechanics tests [14].

We have presented here a typical experiment and a typical numerical simulation. Since the simulated and the tested material were not identical, the numerical simulation should be considered as a qualitative validation and illustration of the methodology, without any attempt to extract accurate values of the dynamic flexural strength.

Future work will concentrate on the practical implementation of the presented methodology on a well defined material for which the statistical nature of the dynamic flexural strength will be assessed.

5. Summary and Conclusions

- A new approach has been proposed to test the dynamic flexural strength of brittle materials.
- An instrumented bar is used to load a small beam specimen in one point, causing its inertial fracture.
- During the test, the prescribed velocity/load and the fracture time are measured.
- These are next used as a boundary condition and failure criterion in a numerical (FE) model of the impacted beam.
- The methodology is simple to implement, both experimentally and numerically, and it does not require testing of large specimens.
- It is believed that the proposed methodology can be applied to large scale testing of brittle materials.

Acknowledgement: The authors acknowledge with gratitude Plasan-Sasa's financial support through grant 2013708.

References

[1] ASTM-C1161. Standard Test Method for Flexural Strength of Advanced Ceramics at Ambient Tepmerature. 1994.

[2] ASTM-C1424. Standard Test Method for Monotonic Compressive Strength of Advanced Ceramics at Ambient Temperature. 1999.

[3] ASTM-C1421. "Standard Test Methods for Determination of Fracture Toughness of Advanced Ceramics at Ambient Temperature". 1999.

[4] Chen WN, Ravichandran G. Dynamic compressive failure of a glass ceramic under lateral confinement. Journal of the Mechanics and Physics of Solids 1997;45:1303.

[5] Timoshenko S, Goodier J. Theory of Elasticity. New York: McGraw-Hill, 1970.

[6] ASTM-C1144. Standard Test Method for Splitting Tensile Strength for Brittle Nuclear Waste Forms. 1989 (reapproved 2004).

[7] Hudson JA. Tensile Strength and Ring Test. International Journal of Rock Mechanics and Mining Sciences 1969;6:91.

[8] Yu Y, Zhang JX, Zhang JC. A modified Brazilian disk tension test. International Journal of Rock Mechanics and Mining Sciences 2009;46:421.

[9] Wang QZ, Li W, Xie HP. Dynamic split tensile test of Flattened Brazilian Disc of rock with SHPB setup. Mechanics of Materials 2009;41:252.

[10] Johnston C, Ruiz C. Dynamic Testing of Ceramics under Tensile-Stress. International Journal of Solids and Structures 1995;32:2647.

[11] Erzar B, Forquin P. An Experimental Method to Determine the Tensile Strength of Concrete at High Rates of Strain. Experimental Mechanics 2009:1.

[12] Dai F, Xia K, Luo SN. Semicircular bend testing with split Hopkinson pressure bar for measuring dynamic tensile strength of brittle solids. Review of Scientific Instruments 2008;79.

[13] Bohme W, Kalthoff JF. The Behavior of Notched Bend Specimens in Impact Testing. International Journal of Fracture 1982;20:R139.

[14] Weisbrod G, Rittel D. A method for dynamic fracture toughness determination using short beams. International Journal of Fracture 2000;104:89.

[15] Rittel D, Pineau A, Clisson J, Rota L. On testing of Charpy specimens using the one-point bend impact technique. Experimental Mechanics 2002;42:247.

[16] Belenky A, Bar-On I, Rittel D. Static and dynamic fracture of transparent nanograined alumina. Journal of the Mechanics and Physics of Solids 2010;58:484.

[17] Delvare F, Hanus JL, Bailly P. A non equilibrium approach to processing Hopkinson Bar bending test data: Application to quasi-brittle materials. International Journal of Impact Engineering;In Press, Accepted Manuscript.

[18] ABAQUS. 2008. p.Dassault Systems.

[19] Giovanola JH. Investigation and Application of the One-Point-Bend Impact Test. ASTM, Philadelphia, PA, USA, 1986. p.307.

[20] Dorogoy A, Rittel D. Transverse impact of free-free square aluminum beams: An experimental-numerical investigation. International Journal of Impact Engineering 2008;35:569.

Tables

Table 1: Material properties that were used for numerical calculations and specimen's geometry optimization.

	Material Name	Density ρ [kg/m^3]	Young's modulus E [GPa]	Poisson's ratio ν	Flexural Strength [MPa]
Incident Bar	15-5 PH steel	7800	204	0.3	-
Specimen (CoorsTek)	Alumina 99.5%	3930	370	0.22	379

Table 2: Mesh properties that were used for assessing the validity of stress distribution.

Mesh type	Element type		Number of elements		Element size h_{el} [mm]		Normalized element size [2] h_{el}^{av}	
							$h_{el}/\phi d$	h_{el}/d
	Incident bar	Specimen	Incident bar	Specimen	Incident bar	Specimen	Incident bar	Specimen
Average	C3D8R[1]		11000	19300	1	0.25	0.157	0.063

Notes:

1. C3D8R – an 8-node linear brick element, reduced integration, hourglass control.
2. $h_{el}^{av} = h_{el}/d$, h_{el} is the element size and d is the depth of ceramic specimen (Figure 1) and ϕd is the diameter of the incident bar.

Figures

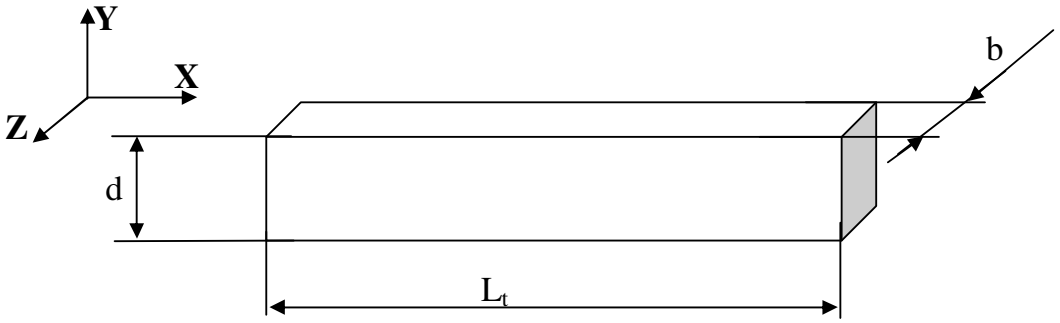

Fig. 1: Specimen dimensions. L_t is the length, b is the width and d is the depth of the ceramic specimens [1].

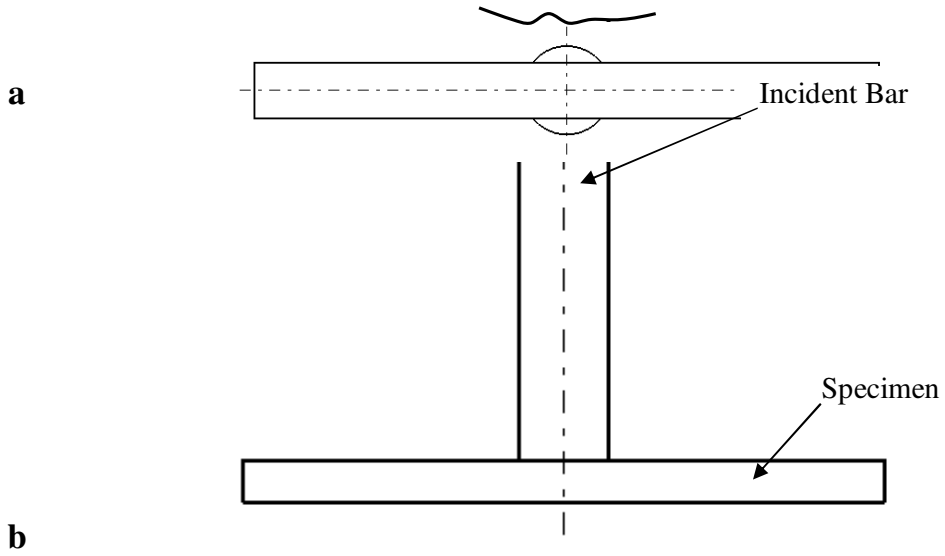

Fig. 2: Schematic drawing of 1-point impact experimental setup. **a**: front view – assembly of the specimen and incident bar. **b**: top view – the specimen lies in contact with the incident bar only.

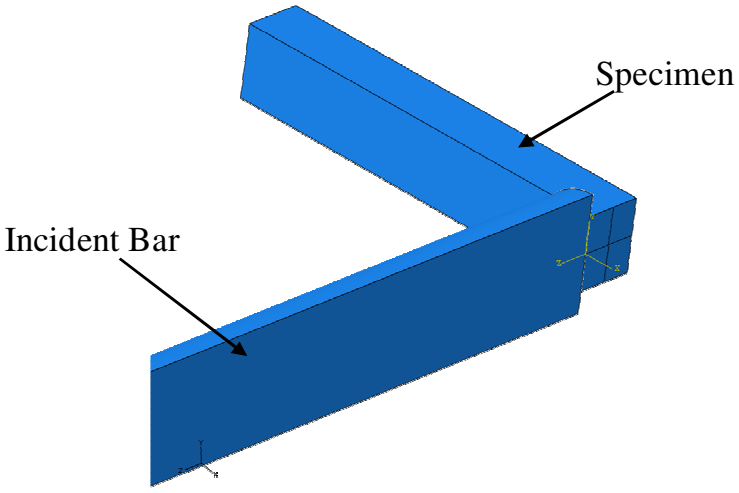

Fig. 3: Close up on 3D model of half-specimen and half of the incident bar that were used to validate the numerical convergence and specimen dimension optimization.

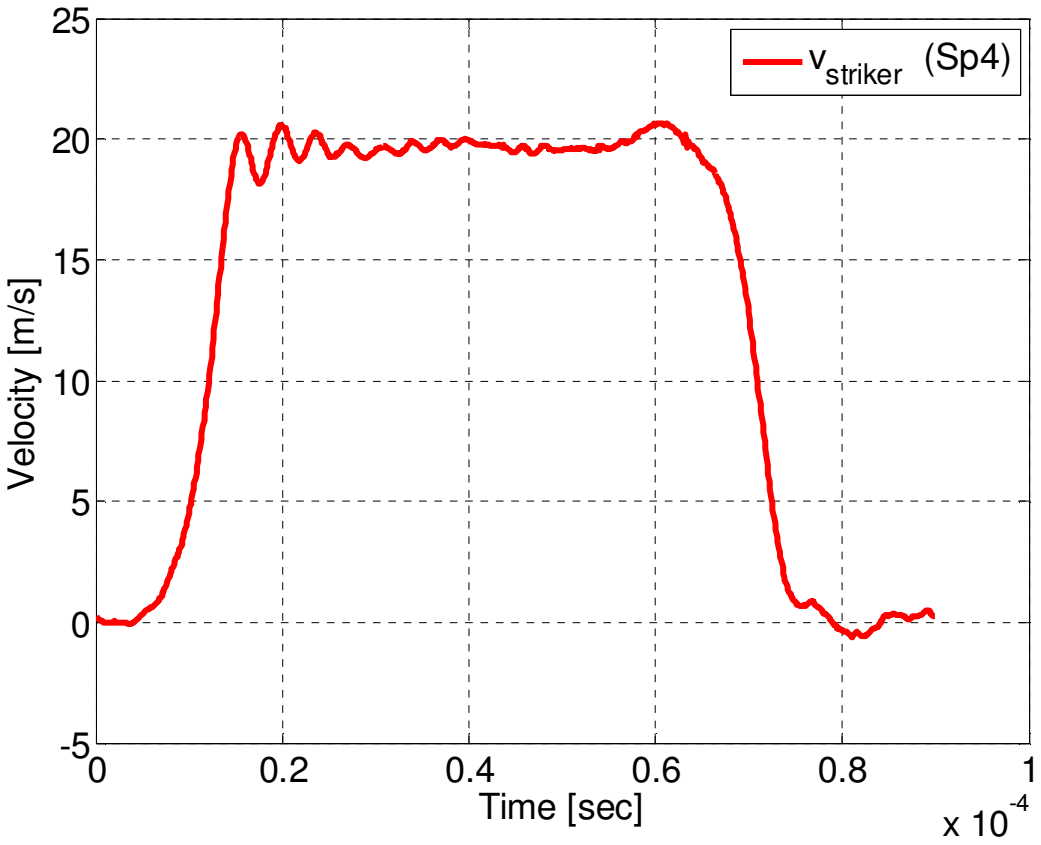

Fig. 4: Velocity profile that was used for numerical simulations and as measured in ordinary 1-point impact test (Sp4).

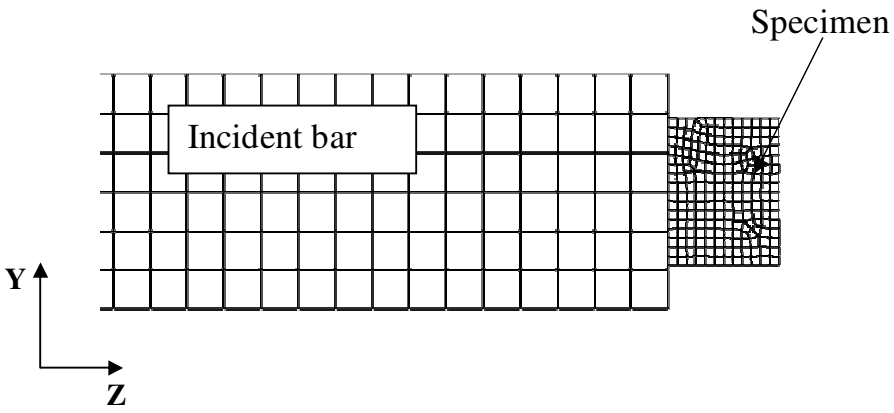

Fig. 5: Close up on meshed incident bar and specimen using one symmetry condition. All other boundary conditions were set free-free as in actual 1-point impact test.

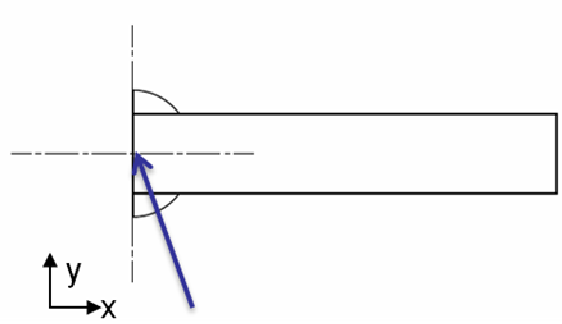

Fig. 6a: The midpoint on outer tensile surface of the specimen where the stress distribution was compared (Figure 6b).

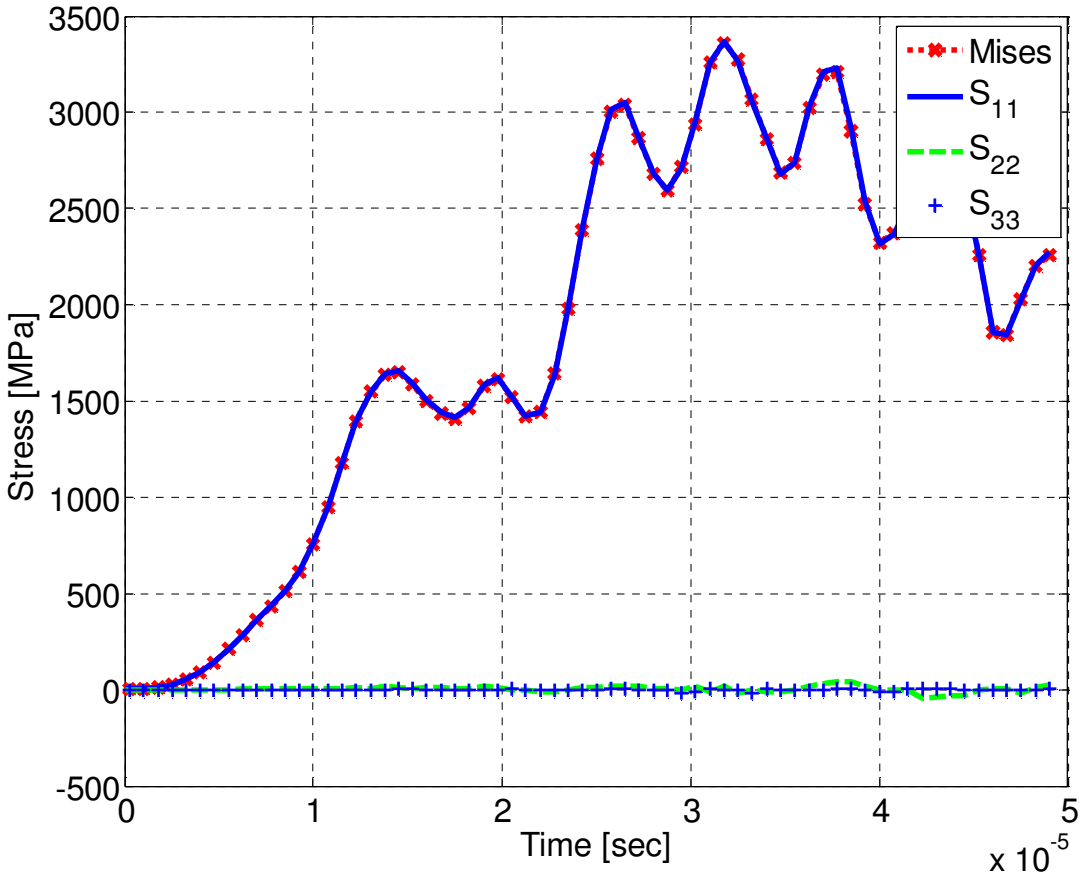

Fig. 6b: Stress distribution on the outer tensile surface of the specimen during 1-point impact simulation. The bending stress (S_{11}) prevails during most time of loading.

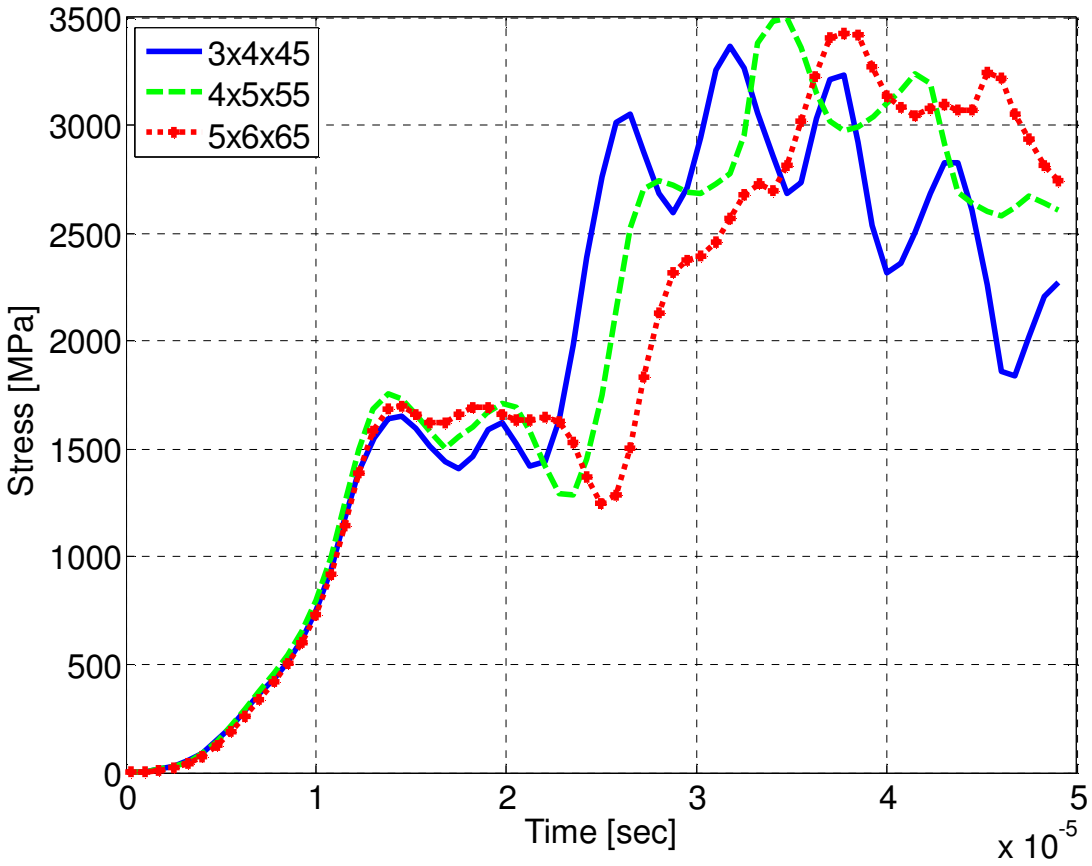

Fig. 7: Bending stress distribution for different specimens' dimensions. For the first ~12 [μs] there is almost no difference between the curves, suggesting that the specimen behaves as infinite during that time.

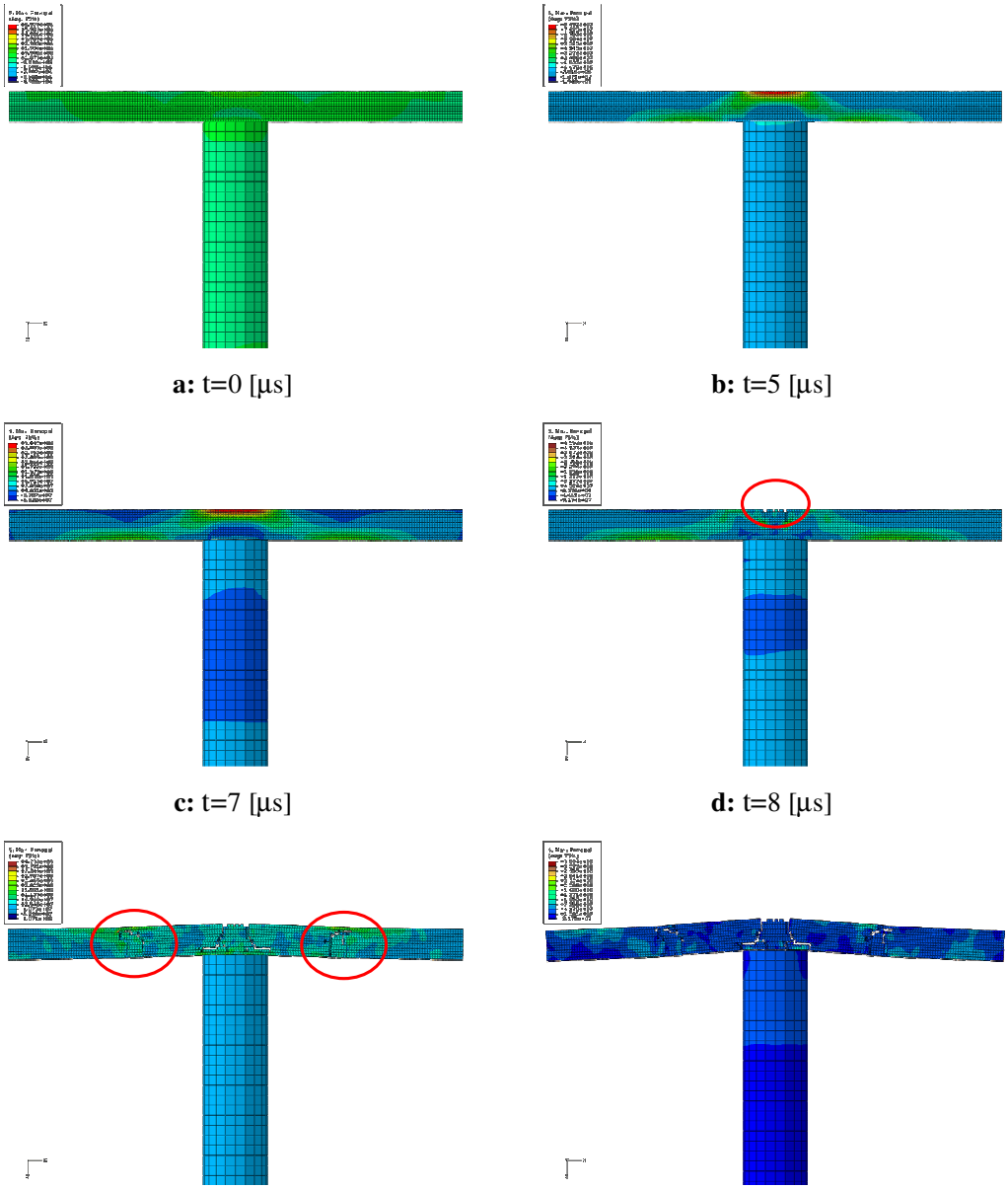

a: t=0 [µs] **b:** t=5 [µs]

c: t=7 [µs] **d:** t=8 [µs]

e: t=18 [µs] **f:** t=29 [µs]

Fig. 8: Numerical failure prediction by maximum principal stress failure criterion. The stress color-map refers to maximum principal stress. **a:** stress wave reaches the specimen, t=0 [µs]; **b-c:** maximum principle stress distribution in the specimen after t=5 and t=7 [µs], respectively; **d:** after t=8 [µs] the specimen fails and the crack(s) initiated from the outer (tensile) surface of the specimen; **e:** additional cracks formed after on both sides of the specimen, t=18 [µs]; **f:** the end of numerical simulation, t=29 [µs].

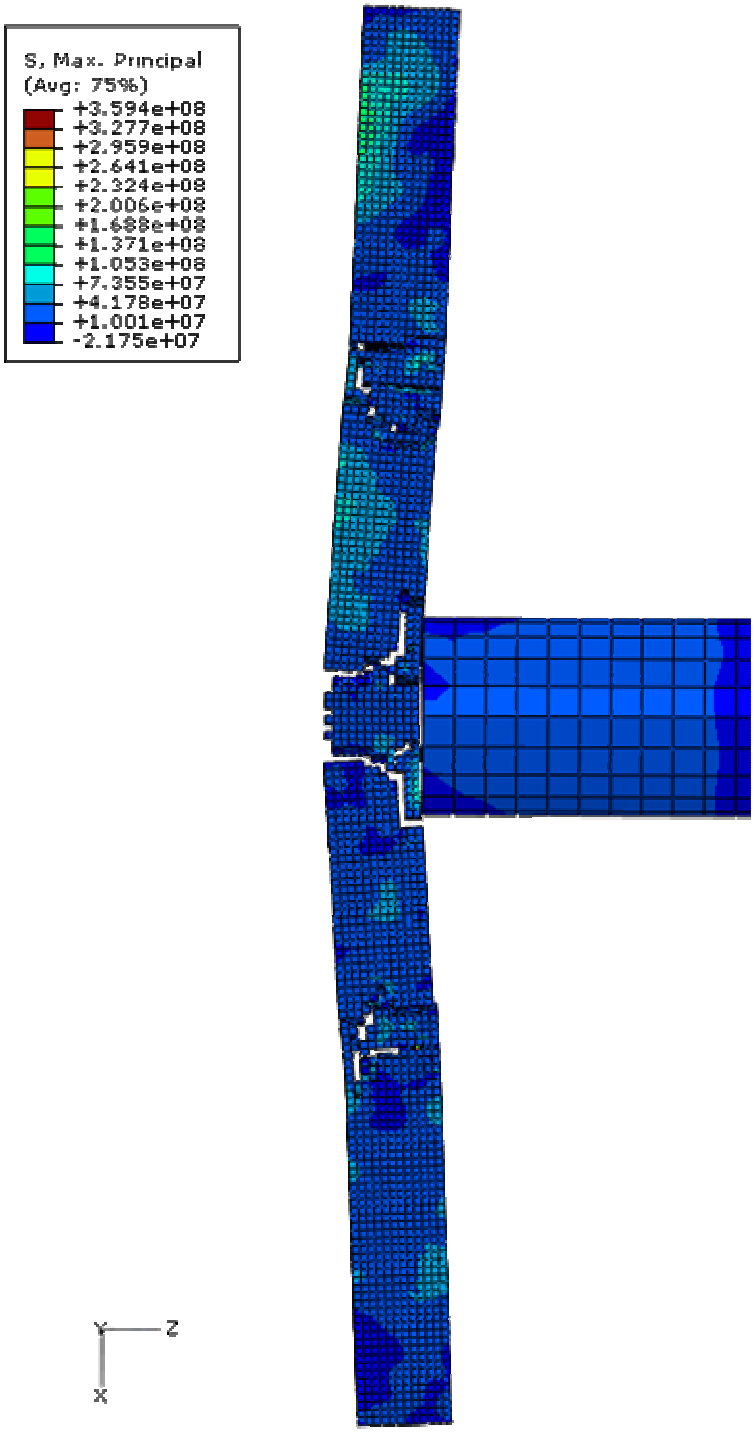

Fig. 9: Close up on the total failure of the specimen, as in Figure 8f, t=29 [μs]. Note the additional cracks on both sides of the specimen.

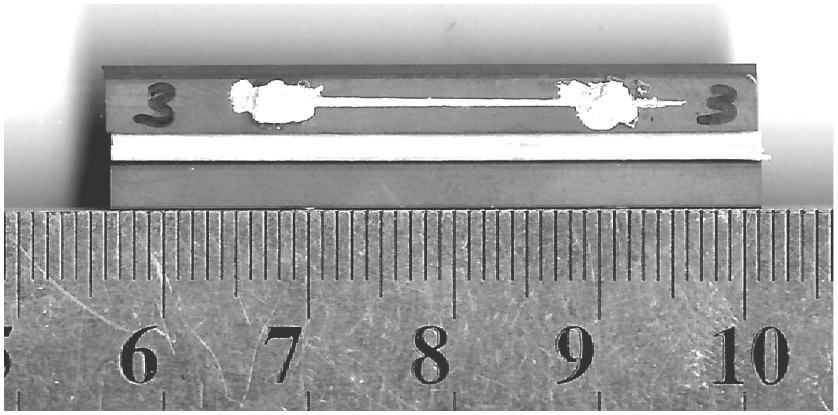

Fig. 10: Short beam specimen, 3x4x45 [mm^3], with silk-screened fracture gauge.

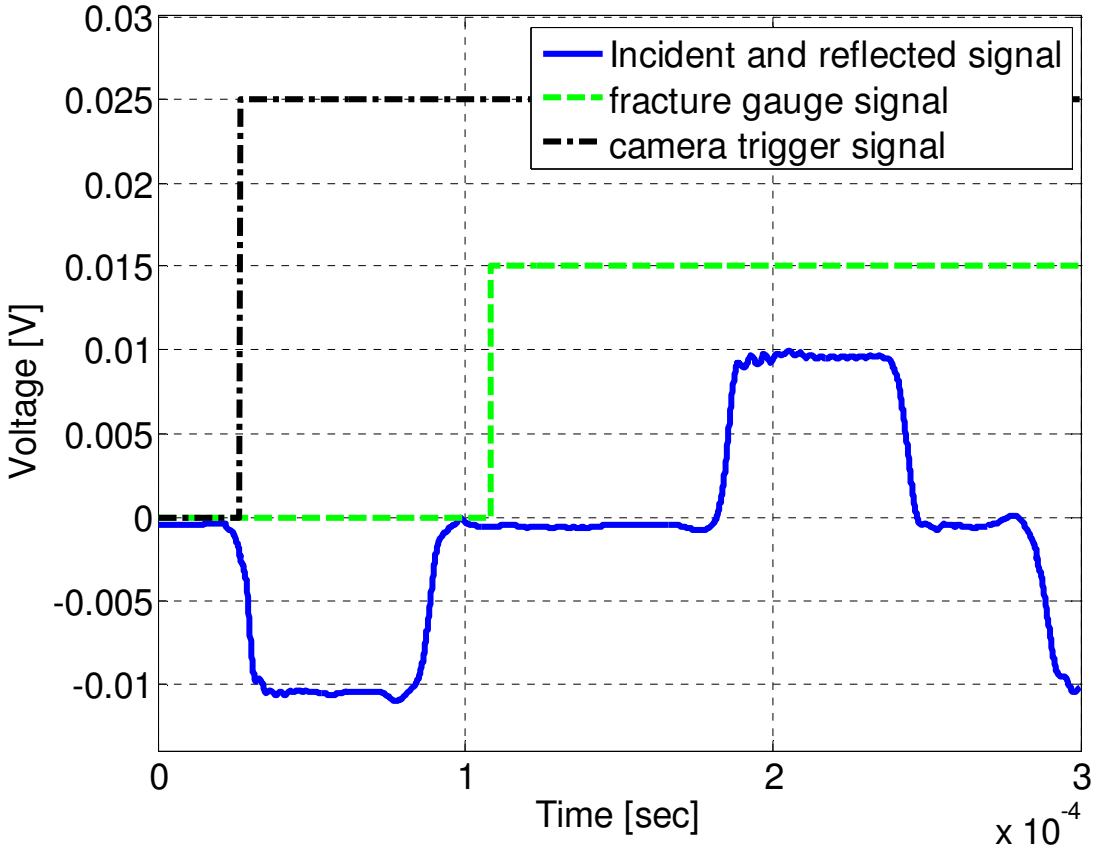

Fig. 11: Raw signals that were recorded during 1-point impact test (Sp4). The fracture gauge and camera trigger were synchronized with the incident pulse.

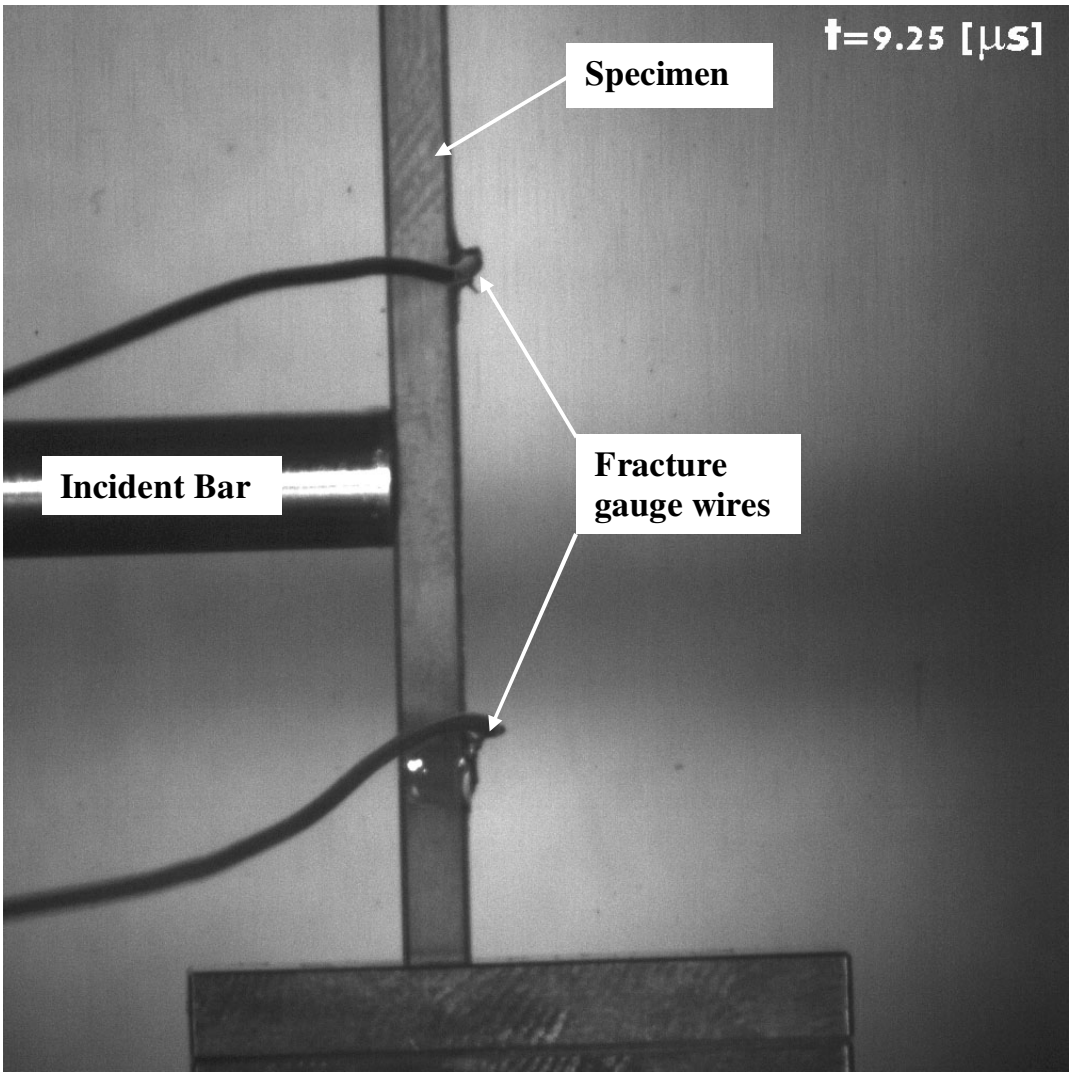

Fig. 12: High-speed picture of one point-impact test (Sp4) at t=9.25 [μs] (after specimen impingement by the stress wave). Failure has not started and the specimen is still in contact with the incident bar.

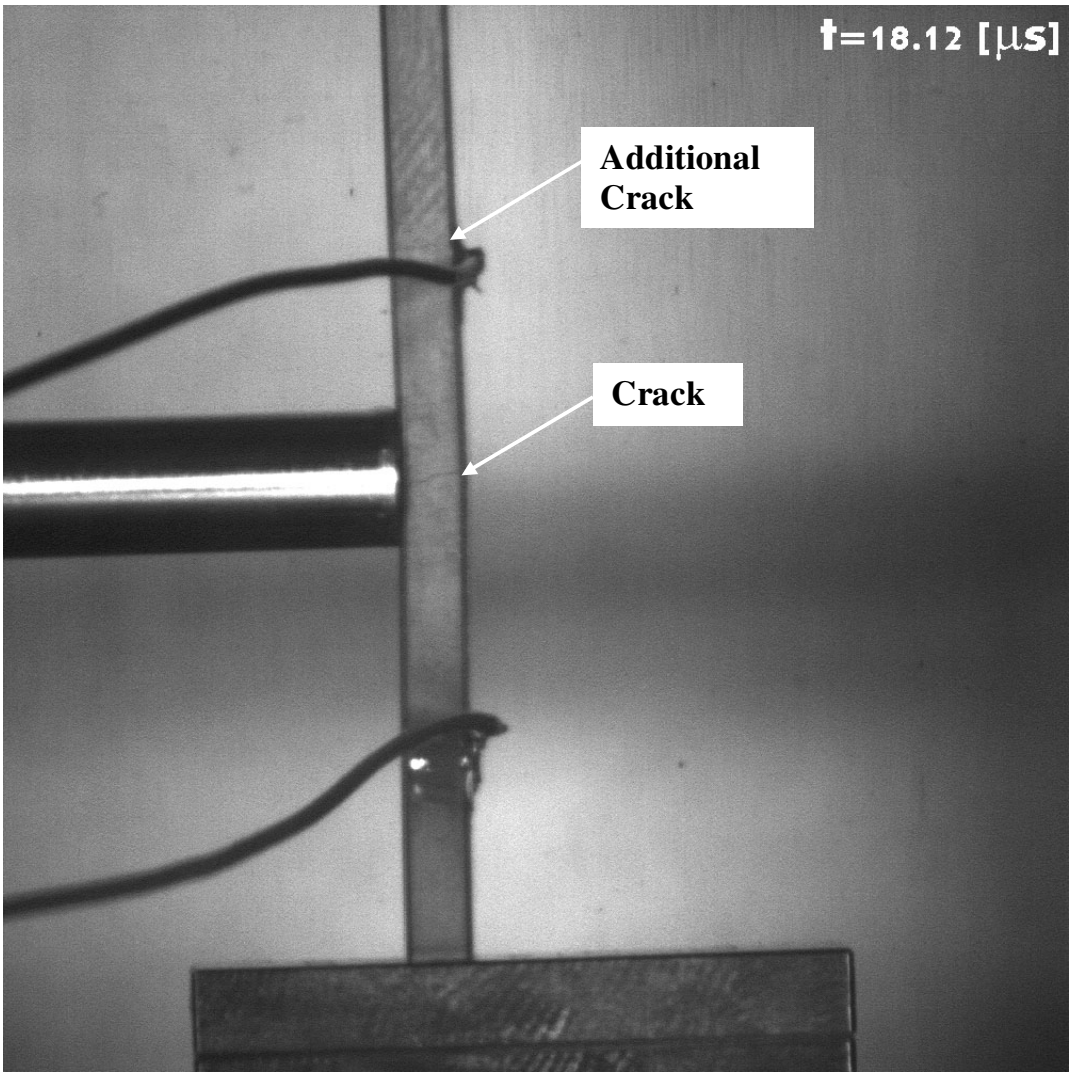

Fig. 13: Second picture in the sequence, t=18.12 [μs]. The specimen is fractured in the middle and an additional crack starts to develop. Fracture gauge reading is t=9.92 [μs].

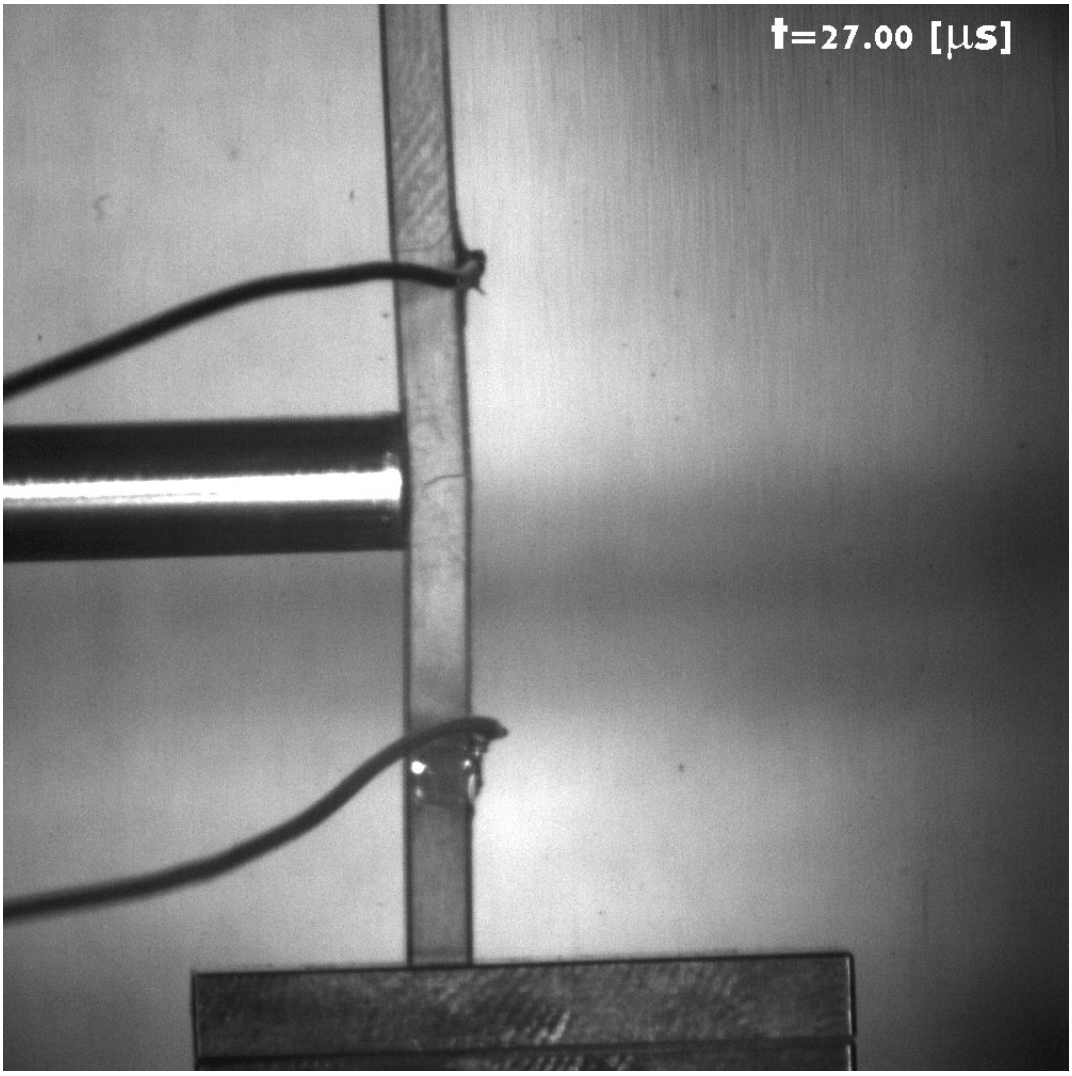

Fig. 14: Third picture in the sequence, t=27.00 [μs], (Sp4). The specimen gets significant bending in the area of contact with the incident bar, but is still in contact with the bar. The additional crack, above the upper tab of the fracture gauge is clearly seen (arrow).

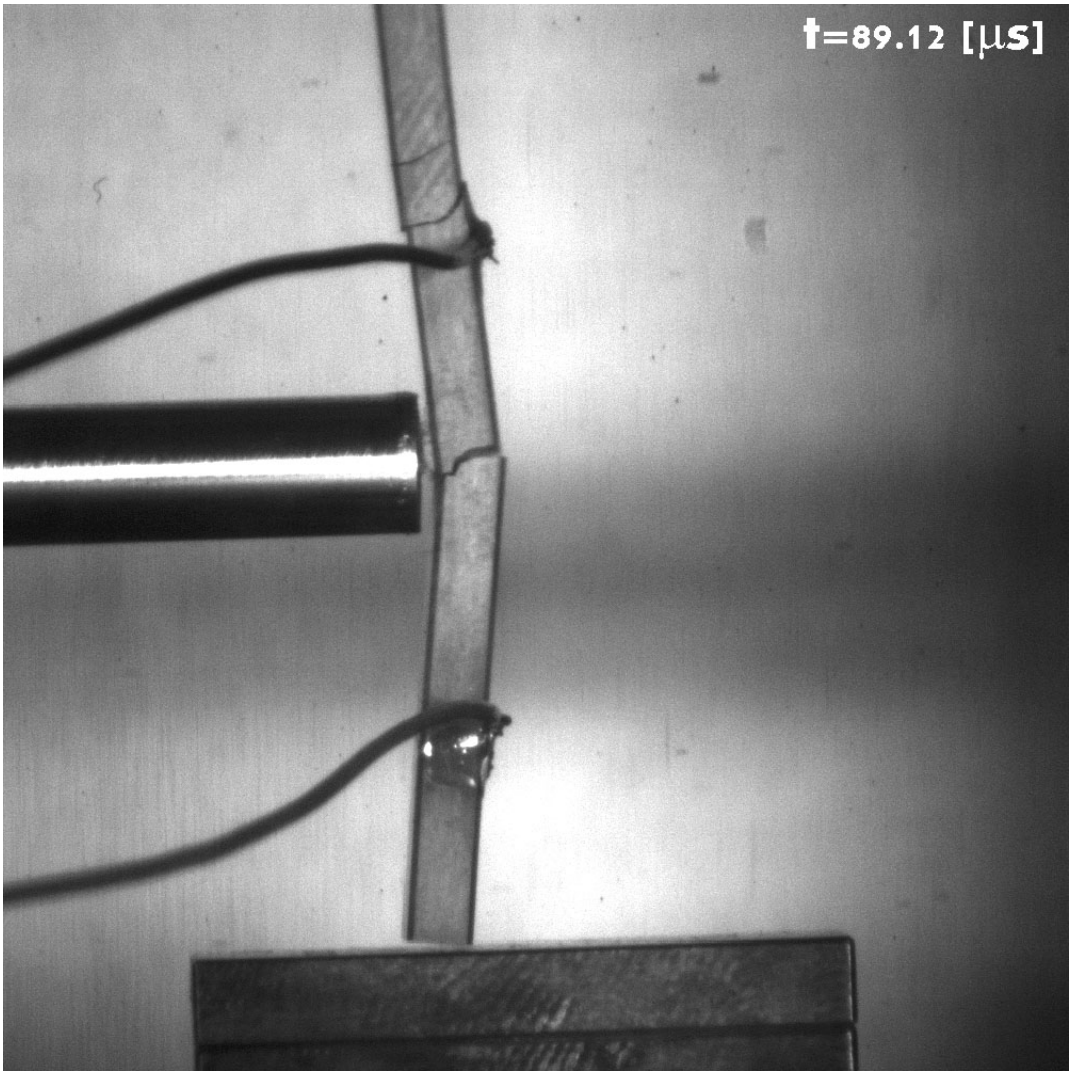

Fig. 15: Total failure and loss of contact for the same specimen, at t=89.12 [μs] (Sp4).